Importance of intersheet scattering in the Hall resistivity of Cd

J. E. A. Alderson, S. P. McAlister, and C. M. Hurd
National Research Council of Canada, Ottawa, Canada K1A 0R9
(Received 10 January 1977)

A sign change of the Hall resistivity $\rho_{21}(T)$ ($\vec{B} \parallel [0001]$) occurs at low temperatures in Cd, Zn, and Mg. In Cd it has been attributed to intersheet scattering, but this explanation does not apply to Zn and Mg. Could an explanation be offered for Cd without invoking intersheet scattering? This paper examines relevant experimental and calculated results, and concludes that intersheet scattering is important in Cd.

Young, Ruvalds, and Falicov[1] suggested that intersheet scattering of electrons at special points on the Fermi surface in the ΓKM plane of Cd could be the cause of the sign change in the Hall resistivity ρ_{21} seen at low temperatures when $\vec{B} \parallel [0001]$. This suggestion has become an established explanation of $\rho_{21}(\vec{B}, T)$ in the low-temperature range,[2-5] although there is an alternative one. A change of sign can be produced from a combination of electronlike and holelike contributions (representing closed orbits on the monster and lens, respectively) without intersheet scattering, as we show below. The question of whether this mechanism is sufficient to explain $\rho_{21}(T)$ in Cd has not been discussed. The following experimental and calculated results suggest it is not sufficient, and intersheet scattering has to be invoked.

The salient features of $\rho_{21}(T)$ in Cd can be reproduced by a path integral calculation using the simplified model Fermi surface of Fig. 1. (This type of calculation has been described in detail elsewhere.[4,5]) Conduction in the basal plane is assumed to be dominated by electrons represented on two pieces of Fermi surface: a trifoliate monster of uniform cross section shown in plan (Fig. 1), and a lens of circular cross section, shown in elevation. The cyclotron orbit of the monster is made up of electronlike arcs, except for the semicircular holelike ones that form the "clover-leaf tips,"[3] while the lens orbit is electronlike. The angular sweep and radius of the arcs is chosen to give a realistic scale model of the orbits based upon the known dimensions of the Fermi surface in the ΓKM plane.[6] The thickness of the trifoliate section ($\Delta k_z = 0.11 \times 10^{10}$ m^{-1}) is chosen to compensate the lens. Interarc transitions of probability[4,5] Q along the dotted paths in Fig. 1 are permitted, where Q is calculated from Young's two-channel expression [Eq. (1.1) of Ref. 1]. Using the arbitrary parameters specified below, the calculation evaluates separately the magnetoconductivity tensor σ_{ij} of the monster and lens for a given temperature. The sum of these tensors is inverted to give the total magnetoresistivity tensor. Throughout the calculation, which is made in absolute units, the direction of the primary current is $[10\bar{1}0]$ and that of $\vec{B}$ (= 2.0 T) is [0001], corresponding to experiment.[4]

The purpose is to show that the main features of the experimental $\rho_{21}(T)$ can be obtained with or without intersheet scattering using values of the model's parameters that are realistic, as far as is known. Four temperature-dependent parameters are involved when intersheet scattering is permitted, and three when it is not. These are $\tau_M(T)$ and $\tau_L(T)$, the relaxation times assigned to the electron arcs on the monster and lens orbits, respectively; $b(T)[=\tau_H(T)/\tau_M(T)]$, the interarc anisotropy[4,5] of the relaxation times on the monster, which thus fixes τ_H, the relaxation time on the semicircular hole arcs forming the clover-leaf tips; and $\Pi(T)$, the two-channel scattering time[1,4,5] required when intersheet scattering is included. We find it necessary to introduce interarc anisotropy on the monster to be able to reproduce the negative tendency of $\rho_{21}(T)$ seen[4] with increasing temperature above ~18 K. This model calculation for conduction in the basal plane of Cd is an improvement upon our earlier one[4] in at least two important respects: firstly, we incorporate the lens and assure electron-hole compensation; and secondly, we use a more realistic geometry for the monster (compare Fig. 1 with Fig. 4 of Ref. 4).

Conforming with experiment,[7] we let both $\tau_M(T)$ and $\tau_L(T)$ take the form $1/\tau(T) = p + qT^n$, where p and q are constants and $n = 3$ for the monster and 5 for the lens. [There seems to be little empirical knowledge to guide the choice of $b(T)$ and $\Pi(T)$, except that the latter must increase with increasing temperature and has previously[1] been assigned values in the range 10^{-10}–10^{-12} sec at low temperatures. Our choice matches both these requirements.] Throughout the calculation, we use the $\tau_M(T)$ and $\tau_L(T)$ shown in Fig. 2. $b(T)$ is varied monotonically between 1.0 at 1 K and 0.78 at 40 K, corresponding to a decrease of the lifetime on the clover-leaf tips relative to that on the main surface of the monster as temperature increases. When intersheet scattering is permitted, $\Pi(T)$ in-

creases monotonically from 4.2×10^{-12} sec at 1 K (corresponding to $Q=0.53$) to 3.4×10^{-9} sec at 8.5 K, at which temperature the intersheet scattering is essentially zero ($Q\approx0$).

Figure 3 compares results obtained with (curve 1) and without (curve 3) intersheet scattering. These are equally good qualitative imitations of the experimental behavior, showing all its salient features.[4] Both curves arise from contributions of the orbit on the monster and the circular electron orbit on the lens. In the case of curve 3, the monster orbit is just the closed trifoliate one shown in the upper part of Fig. 1, which has a net holelike response in the high-field condition.[1-5] In the case of curve 1, the monster orbits are more complicated since intersheet scattering gives a nonzero probability to electronlike paths such as A or E in Fig. 4 of Ref. 5, which dominate the behavior below about 7 K. This can be seen from curve 2, which is the behavior when the intersheet scattering is turned off ($Q=0$) in the circumstances of curve 1. The difference between curves 1 and 2 is thus the consequence of the intersheet scattering. The dotted curves in Fig. 3 are the corresponding behaviors when the lens orbit is eliminated. In the case with intersheet scattering [Fig. 3(a)], the same qualitative shape of $\rho_{21}(T)$ is maintained, showing that the sign change arises from the monster's contribution (as proposed previously[1-5]), but in the case without intersheet scattering $\rho_{21}(T)$ no longer resembles experiment when the lens is removed.

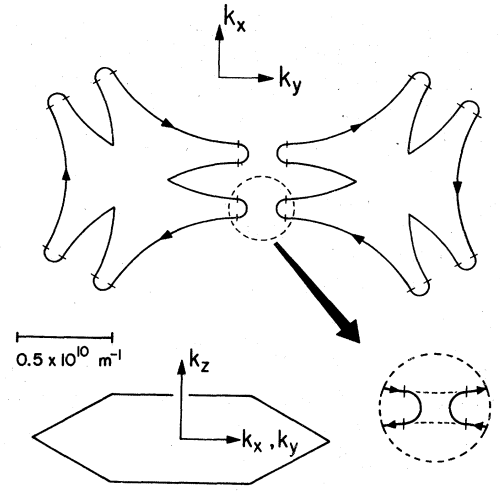

FIG. 1. Scale drawing in reciprocal space showing the model cyclotron orbits used in the path integral calculation; $\vec{B}\|k_z$. The upper part shows a plan view of the trifoliate monster surface, with intersheet transitions permitted between tips as shown dotted in the inset. The lower part shows the circular lens surface in elevation.

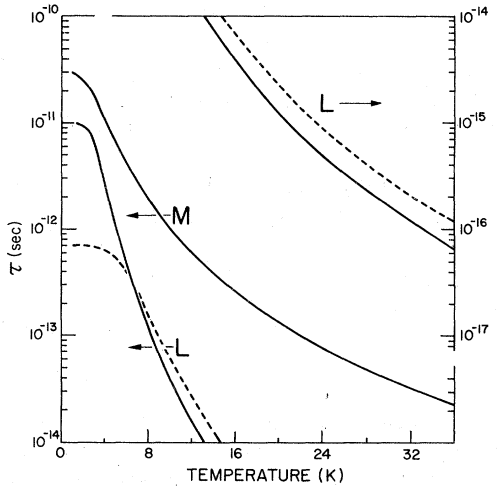

FIG. 2. Temperature dependence of the relaxation times assigned to the electron arcs on the monster (M) and lens (L). The dotted line is $\tau_L(T)=0.7/(10^4+T^5)\times10^{-8}$ sec used when intersheet scattering is allowed (curve 1 of Fig. 3), and the solid line is $\tau_L(T)=1/(9.97\times10^2+2.58\,T^5)\times10^{-8}$ sec used with no intersheet scattering (curve 3 of Fig. 3); $\tau_M(T)=1/(324+9.68T^3)\times10^{-8}$ sec is common to both cases. The $\tau_L(T)$ variations are essentially equivalent except below ~7 K. In that range, the larger τ_L values are required when there is no intersheet scattering to assure that transition of the lens orbit to the high-field condition, and hence the sign change of $\rho_{21}(T)$.

Figure 3 raises the question of whether intersheet scattering is needed to explain the observed $\rho_{21}(T)$ of Cd, or whether the observed behavior arises from closed electron and hole orbits as in

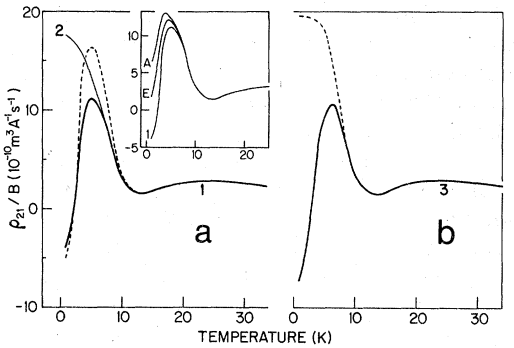

FIG. 3. Thicker lines show the temperature dependence of the Hall resistivity (divided by the applied flux density, where $\vec{B}=2.0T$) obtained with the model of Fig. 1. Curve 1 is a case with intersheet scattering while curve 3 is one without, showing that in both cases the qualitative behavior found experimentally can be imitated (Fig. 2 of Ref. 4). Curves A and E are, respectively, the behaviors when the A and E orbits (Fig. 4 of Ref. 5) are eliminated in the circumstances of curve 1.

Fig. 3(b). We think the results of Fig. 4 suggest an answer. They show that $\rho_{21}(T)$ for similar monocrystals of Cd and Zn depends very differently upon the sample's thermal history. The curves A are the behaviors previously published for the samples in the "as-grown" condition.[4,5,8] Curve B is the behavior for Cd after annealing at 403 K for 250 h, while curves $1 \rightarrow 5$ are new results showing the behaviors seen as the sample is given increasing amounts of cold work by repeatedly quenching it from room temperature into liquid N_2. (Details are given in the caption.) The resistance ratio (RRR) of the sample was insensitive to this treatment; no change could be detected in it with the treatment leading from B to curve 3 of Fig. 4, even though the $\rho_{21}(T)$ changed markedly. When the same treatment is given to Zn, there is no large change in $\rho_{21}(T)$. All the behaviors fall within a narrow range (labeled 1 in Fig. 4) that barely differs from the as-grown behavior. The RRR of the Zn sample was also insensitive to the repeated quenching.

We suggest that this contrast between Zn and Cd in the sensitivity of their $\rho_{21}(T)$ at low temperature to cold work shows that the Hall effect is dominated by different influences in the two metals. In Cd the sign change of $\rho_{21}(T)$ could arise from the imbalance between the contributions from closed electron and hole orbits, as in Fig. 3(b). But the sensitivity of $\rho_{21}(T)$ to the small-angle scattering of dislocations introduced by the internal strain of quenching suggests the existence of a large scattering-dependent component in the galvanomagnetic tensor, such as that produced by intersheet scattering.[9] Thus as the dislocation density is increased and with it the total amount of small-angle scattering, so we expect a decrease in Π at any given temperature[4] leading to an increase in the intersheet scattering probability Q. Hence, $\rho_{21}(T)$ at a given low temperature becomes increasingly negative as the number of successive quenches is increased (Fig. 4). [Although Fig. 3 shows that a sign change of $\rho_{21}(T)$ can be produced by competitive contributions from closed electron and hole orbits, this is probably not the mechanism producing the behavior of ρ_{21} for Zn (Fig. 4) or Mg,[10] where intersheet scattering is not involved. The effect of magnetic breakdown in the basal plane has to be considered in the latter cases.[3,10]]

The experimental support (Fig. 4) for the importance of intersheet scattering in Cd means that the model leading to Fig. 3(a) is the preferred description. We can use it to investigate artificial circumstances of interest. Intersheet scattering leads to electron orbits of types A and E (Fig. 4 of Ref. 5) in the ΓKM plane. When these orbits reach

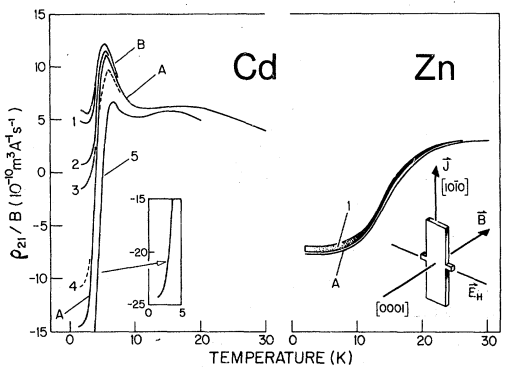

FIG. 4. Comparison of the effect of the sample's thermal history upon the Hall resistivity $\rho_{21}(T)$ for similar samples of Cd and Zn aligned as in the sketch. Curves A are the as-grown behaviors ($\rho_{273K}/\rho_{1.7K}$ = 25 600 for Cd and 17 831 for Zn). Curve B is the behavior after annealing at 403 K for 250 h. Curves $1 \rightarrow 5$ for Cd are the behaviors after a total of 3, 7, 11, 16, and 47 successive quenches from room temperature into liquid N_2. A similar treatment of the Zn sample produced barely any change from the as-grown behavior, with the behaviors of the annealed and multiply quenched states lying within the region labeled 1. The experimental details are the same as those given in Refs. 4 and 8.

the high-field condition[1-5] the compensation is destroyed, shifting $\rho_{21}(T)$ to more negative values and eventually changing its sign [Fig. 3(a)]. Previously[1-4] this has been attributed to the effect of the "giant orbit" A, although the completion of this orbit is less probable in given circumstances than that of E because the latter requires fewer successive intersheet scatterings. The inset in Fig. 3 shows the result of eliminating separately the A and E orbits. Both sets of orbits are evidently important in producing the sign change in the simulated behavior of $\rho_{21}(T)$. Because of its simplified geometry, our previous calculation[4] did not include the E orbits.

We conclude that the importance of intersheet scattering in the basal plane of Cd is supported by the above experimental and calculated results. As a result of this scattering, electron orbits of type A and E (Fig. 4 of Ref. 5) are completed in the high-field condition and both make an important contribution to the breakdown of compensation leading to the sign change of $\rho_{21}(T)$.

ACKNOWLEDGMENTS

We thank G. F. Turner for the care given to the preparation of the monocrystals, and L. D. Calvert for making available his x-ray facilities.

[1]R. A. Young, J. Ruvalds, and L. M. Falicov, Phys. Rev. 178, 1043 (1969).
[2]O. P. Katyal and A. N. Gerritsen, Phys. Rev. 178, 1037 (1969).
[3]D. A. Lilly and A. N. Gerritsen, Phys. Rev. B 9, 2497 (1974); Physica (Utr.) 69, 286 (1973); A. N. Gerritsen, Phys. Rev. B 10, 5232 (1974); 12, 4247 (1975).
[4]C. M. Hurd, J. E. A. Alderson, and S. P. McAlister, Phys. Rev. B 14, 395 (1976).
[5]J. E. A. Alderson, C. M. Hurd, and S. P. McAlister, Can. J. Phys. 54, 1866 (1976).
[6]R. C. Jones, R. G. Goodrich, and L. M. Falicov, Phys. Rev. 174, 672 (1968).
[7]P. D. Hambourger, in *Proceedings of the Thirteenth International Low Temperature Physics Conference, Boulder, Colorado, 1972*, edited by R. H. Kropschot and K. D. Timmerhaus (University of Colorado, Boulder, Colo., 1973), p. 278.
[8]C. M. Hurd, J. E. A. Alderson, and S. P. McAlister, Can. J. Phys. 55, 620 (1977).
[9]The sensitivity of ρ_{21} in Cd in quenching to cryogenic temperatures may be the cause of the unexplained irreproducibility found previously by Lilly and Gerritsen (Ref. 3) for $\rho_{21}(T)$ of samples of apparently equivalent purity and thermal history.
[10]S. P. McAlister, J. E. A. Alderson, and C. M. Hurd (unpublished).